

Measurement of the Ratio of Branching Fractions $\mathcal{B}(B_c^+ \rightarrow J/\psi\tau^+\nu_\tau)/\mathcal{B}(B_c^+ \rightarrow J/\psi\mu^+\nu_\mu)$

R. Aaij *et al.**
(LHCb Collaboration)

 (Received 16 November 2017; revised manuscript received 19 January 2018; published 23 March 2018; corrected 4 April 2018)

A measurement is reported of the ratio of branching fractions $\mathcal{R}(J/\psi) = \mathcal{B}(B_c^+ \rightarrow J/\psi\tau^+\nu_\tau)/\mathcal{B}(B_c^+ \rightarrow J/\psi\mu^+\nu_\mu)$, where the τ^+ lepton is identified in the decay mode $\tau^+ \rightarrow \mu^+\nu_\mu\bar{\nu}_\tau$. This analysis uses a sample of proton-proton collision data corresponding to 3.0 fb^{-1} of integrated luminosity recorded with the LHCb experiment at center-of-mass energies of 7 and 8 TeV. A signal is found for the decay $B_c^+ \rightarrow J/\psi\tau^+\nu_\tau$ at a significance of 3 standard deviations corrected for systematic uncertainty, and the ratio of the branching fractions is measured to be $\mathcal{R}(J/\psi) = 0.71 \pm 0.17(\text{stat}) \pm 0.18(\text{syst})$. This result lies within 2 standard deviations above the range of central values currently predicted by the standard model.

DOI: 10.1103/PhysRevLett.120.121801

Semileptonic b -hadron decays provide powerful probes for testing the standard model (SM) and for searching for the effects of physics beyond the SM. Because of their relatively simple theoretical description via tree-level processes in the SM, these decay modes serve as an ideal setting for examining the universality of the couplings of the three charged leptons in electroweak interactions. Recent measurements of the parameters $\mathcal{R}(D)$ and $\mathcal{R}(D^*)$ corresponding to the ratios of branching fractions $\mathcal{B}(B \rightarrow D^{(*)}\tau^-\bar{\nu}_\tau)/\mathcal{B}(B \rightarrow D^{(*)}\mu^-\bar{\nu}_\mu)$ by the BABAR [1,2], Belle [3–6], and LHCb [7–9] Collaborations indicate larger values than the SM predictions [10]. Proposed explanations for these discrepancies include extensions of the SM that involve enhanced weak couplings to third-generation leptons and quarks, such as interactions involving a charged Higgs boson [11,12], leptoquarks [13], or new vector bosons [14]. Furthermore, other hints of the failure of lepton flavor universality have been seen in electroweak loop-induced B -meson decays [15,16].

Measurements of semitauonic decays of other species of b hadrons can provide additional handles for investigating the sources of theoretical and experimental uncertainties and potentially the origin of lepton nonuniversal couplings. This Letter presents the first study of the semitauonic decay $B_c^+ \rightarrow J/\psi\tau^+\nu_\tau$ and a measurement of the ratio of branching fractions

$$\mathcal{R}(J/\psi) = \frac{\mathcal{B}(B_c^+ \rightarrow J/\psi\tau^+\nu_\tau)}{\mathcal{B}(B_c^+ \rightarrow J/\psi\mu^+\nu_\mu)} \quad (1)$$

*Full author list given at the end of the article.

Published by the American Physical Society under the terms of the [Creative Commons Attribution 4.0 International license](https://creativecommons.org/licenses/by/4.0/). Further distribution of this work must maintain attribution to the author(s) and the published article's title, journal citation, and DOI. Funded by SCOAP³.

for which the central values of the current SM predictions are in the range of 0.25–0.28, where the spread arises from the choice of modeling approach for form factors [17–20]. Here and throughout the Letter, charge-conjugate processes are implied.

The measurement is performed using data recorded with the LHCb detector at the Large Hadron Collider in 2011 and 2012, corresponding to integrated luminosities of 1 and 2 fb^{-1} collected at proton-proton (pp) center-of-mass energies of 7 and 8 TeV, respectively. The analysis procedure is designed to identify both the signal decay chain $B_c^+ \rightarrow J/\psi\tau^+\nu_\tau$ and the normalization mode $B_c^+ \rightarrow J/\psi\mu^+\nu_\mu$, with $J/\psi \rightarrow \mu^+\mu^-$ and $\tau^+ \rightarrow \mu^+\nu_\mu\bar{\nu}_\tau$, through their identical visible final states $(\mu^+\mu^-)\mu^+$. The muon candidate not originating from the J/ψ is referred to as the *unpaired* muon. The two modes are distinguished using differences in their kinematic properties. The selected sample contains contributions from the signal and the normalization modes, as well as several background processes. The contributions of the various components are determined from a multidimensional fit to the data, where each component is represented by a template distribution derived from control data samples or from simulation validated against control regions in data. The selection and fit procedures are developed without knowledge of the signal yield (blinded).

The LHCb detector is a single-arm forward spectrometer covering the pseudorapidity range $2 < \eta < 5$ described in detail in Refs. [21,22]. Notably for this analysis, muons are identified by a system composed of alternating layers of iron and multiwire proportional chambers [23]. The on-line event selection is performed by a trigger [24], which in this case consists of a hardware stage based on information from the calorimeter and muon systems, followed by a software stage, which applies a full event reconstruction. Simulated data samples, which are used for producing fit templates and evaluating the signal-to-normalization

efficiency ratio, are produced using the software described in Refs. [25–28].

Events containing a $J/\psi\mu^+$ candidate are required to have been selected by the LHCb hardware dimuon trigger. In the software trigger, the events are required to meet criteria designed to select $J/\psi \rightarrow \mu^-\mu^+$ candidates constructed from oppositely charged tracks whose particle identification information is consistent with a muon. The J/ψ candidate must have $(p_T) > 2 \text{ GeV}/c$, where p_T is the component of the momentum transverse to the beam, and have a reconstructed mass consistent with the known J/ψ mass [29]. In addition, the momenta of the J/ψ decay products must each exceed $5 \text{ GeV}/c$, and at least one muon candidate must have $p_T > 1.5 \text{ GeV}/c$. In the off-line reconstruction, the decay products of the J/ψ candidate must match the muon candidates responsible for the trigger.

Further requirements are imposed in the off-line selection, including ones imposed to ensure good-quality tracks. The J/ψ candidate is required to have well-identified muon decay products, a decay vertex significantly separated from any primary vertex (PV) in the event, and an invariant mass within $55 \text{ MeV}/c^2$ of the known J/ψ mass. A veto is applied to exclude candidates in which the invariant mass of the opposite-sign muon pair formed by swapping the unpaired muon with a muon from the J/ψ candidate is consistent with the J/ψ mass. The unpaired muon candidate must have $p_T > 750 \text{ MeV}/c$ and be significantly separated from any PV. It is required to satisfy muon identification criteria, have a momentum in the range $3 < p < 100 \text{ GeV}/c$, and be in the pseudorapidity range 2–5. The J/ψ candidate and unpaired muon are required to form a vertex with the J/ψ candidate using loose criteria to reduce any inefficiency due to the $J/\psi\text{--}\mu^+$ separation induced by the τ^+ flight in the signal decay. To suppress combinatorial background constructed from the decay products of the other b hadrons in the event, the J/ψ and the unpaired μ candidates must not have momenta pointing in nearly opposite directions in the plane transverse to the beam axis. In the rare ($< 2\%$) events where more than one candidate is selected, a single candidate is retained randomly but reproducibly.

The $J/\psi\mu^+$ candidates from partially reconstructed b -hadron decays, including B_c^+ decays to a $J/\psi H_c$ pair, where H_c stands for a charmed hadron, and semileptonic $B_c^+ \rightarrow J/\psi(n\pi)\mu^+\nu_\mu$ decays with $n \geq 2$ are typically accompanied by additional nearby charged particles. In order to suppress these background contributions, candidates are required to be isolated from additional tracks in the event based on a boosted decision tree (BDT) described in Ref. [7]. The algorithm assigns a score based on whether a given track is likely to have originated from the signal B_c^+ candidate or from the rest of the event. The signal sample is constructed by requiring that no tracks in the event are consistent with originating from the B_c^+ candidate based on their BDT

response value and is, thus, enriched in $B_c^+ \rightarrow J/\psi\tau^+\nu_\tau$ and $B_c^+ \rightarrow J/\psi\mu^+\nu_\mu$ decays.

The selection efficiencies for the signal and normalization modes are determined from simulation. To account for the effect of differing detector occupancy and resolution between simulation and data, the joint distributions of the track multiplicity and the significances of the separation of the J/ψ and of the unpaired muon from the associated PV (defined to be the PV with respect to which the particle under consideration has the smallest impact parameter χ^2 , which is the difference in χ^2 of the PV fit with and without the particle in question) in the simulated samples are weighted to match the observed distribution in a subset of the data sample enriched in the normalization mode, without biasing the distribution of the simulated decay time (i.e., the proper time elapsed between the production and decay of the B_c^+ meson) [30]. This subset is created by excluding events with positive missing mass or long decay times and increasing the rejection of partially reconstructed events using the isolation BDT. The ratio of the signal efficiency to that of the normalization mode in the nominal selection is found to be $(52.4 \pm 0.4)\%$, where the uncertainty reflects the limited size of the simulation samples.

The differences in the kinematic distributions of the various processes are exploited to disentangle their respective contributions to the selected $J/\psi\mu^+$ sample. The large $\mu\text{--}\tau$ mass difference and the presence of extra neutrinos from the decay $\tau^+ \rightarrow \mu^+\nu_\mu\bar{\nu}_\tau$ result in distinct distributions for the signal relative to the normalization mode. Three kinematic quantities are used: the unpaired-muon energy in the B_c^+ rest frame E_μ^* , the missing mass squared defined as $m_{\text{miss}}^2 = (p_{B_c^+} - p_{J/\psi} - p_\mu)^2$, and the squared four-momentum transfer to the lepton system $q^2 = (p_{B_c^+} - p_{J/\psi})^2$, where $p_{B_c^+}$, $p_{J/\psi}$, and p_μ are the four-momenta of the B_c^+ meson, the J/ψ meson, and the unpaired muon, respectively. These quantities are approximated using a technique developed in Ref. [7] that estimates the B_c^+ momentum despite the presence of one or more missing neutrinos, using the flight direction of the candidate determined from the vector joining the associated PV and the decay vertex, and the momenta of its decay products. The lifetime of the B_c^+ meson, which is nearly 3 times shorter than that of other b hadrons, provides an additional handle for discriminating against the large background that originates from lighter b hadrons. The decay time for each $J/\psi\mu^+$ candidate is approximated using the decay distance of the candidate determined from the approximated B_c^+ momentum vector and the displacement of its reconstructed vertex relative to its associated PV.

The contributions of various components to the sample of $J/\psi\mu^+$ candidates are represented by three-dimensional histogram templates binned in m_{miss}^2 , the decay time of the B_c^+ candidate, and a categorical quantity Z representing eight bins in (E_μ^*, q^2) . The values 0–3 of Z correspond to bins where $q^2 < 7.15 \text{ GeV}^2/c^4$ and E_μ^* is divided with

thresholds at [0.68, 1.15, 1.64] GeV. The values 4–7 correspond to bins with the same E_μ^* ranges but where $q^2 \geq 7.15 \text{ GeV}^2/c^4$. These multidimensional histograms reflect nontrivial correlations among the three quantities. The sources of the components represented in the fit and the procedures used to obtain their corresponding templates from simulation and data are outlined below.

The templates are derived from simulation for the signal and the normalization modes, which requires knowledge of the $B_c^+ \rightarrow J/\psi \ell^+ \nu_\ell$ form factors. These have not yet been precisely determined, and the theoretical predictions, e.g., those from Refs. [18,31], are yet to be tested against experiment. Thus, for this measurement, the shared form factors for the signal and normalization modes are determined directly from the data by employing a z -expansion parametrization inspired by Ref. [32] to fit a subsample of the data excluding events with missing mass greater than $1 \text{ GeV}^2/c^4$. In this expansion, the form factors $V(q^2)$, $A_0(q^2)$, $A_1(q^2)$, and $A_2(q^2)$ (following the convention of Ref. [31]) are fit by functions of the form

$$f(q^2) = \frac{1}{1 - q^2/M_{\text{pole}}^2} \sum_{k=0}^K a_k z(q^2)^k, \quad (2)$$

where $z(q^2)$ is defined in Ref. [32]. The pole mass M_{pole} is the mass of the excited B_c^+ state with quantum numbers corresponding to the form factor: the $J^P = 1^-$ state for the form factor $V(q^2)$ taken to be $6.33 \text{ GeV}/c^2$, the 0^- state for $A_0(q^2)$, which is the B_c^+ mass itself, and finally, the 1^+ state for $A_1(q^2)$ and $A_2(q^2)$ taken to be $6.73 \text{ GeV}/c$ [18,31]. The form factor $A_2(q^2)$ is fit to $K = 0$ order, while the others are fit to the linear $K = 1$ order. The parameters a_k obtained from this procedure contain the effects of the reconstruction resolution of the kinematic parameters and cannot be directly compared with existing theoretical predictions.

Simulation is used to determine the templates for the feed-down processes $B_c^+ \rightarrow \psi(2S)\mu^+\nu_\mu$, $B_c^+ \rightarrow \psi(2S)\tau^+\nu_\tau$, $B_c^+ \rightarrow \chi_{c1}\mu^+\nu_\mu$, and $B_c^+ \rightarrow \chi_{c2}\mu^+\nu_\mu$, and backgrounds from $B_c^+ \rightarrow J/\psi H_c X$. The last is represented by a cocktail of decays that result from $b \rightarrow c\bar{c}s$ transitions. The branching fractions for the decays $J/\psi \rightarrow \mu^+\mu^-$, $\psi(2S) \rightarrow J/\psi X$, $\chi_{c(1,2)} \rightarrow J/\psi\gamma$, and $\tau^+ \rightarrow \mu^+\nu_\mu\bar{\nu}_\tau$ are fixed to the known values [29]. A possible feed-down contribution from $B_c^+ \rightarrow X(3872)\mu^+\nu_\mu$, where the $X(3872)$ state decay produces a J/ψ , is considered in the determination of the systematic uncertainties. The semimuonic B_c^+ decays to the χ_{c1} and χ_{c2} modes are constrained to have the same branching fractions relative to the normalization mode, differing only due to the respective branching fractions of $\chi_{c(1,2)}$ to $J/\psi\gamma$, consistent with theoretical expectations [33]. The form factors for these decays are taken from Ref. [33]. The rare decay $B_c^+ \rightarrow \chi_{c0}\mu^+\nu_\mu$ (suppressed by the low $\chi_{c0} \rightarrow J/\psi X$ branching fraction) and semitaonic decays involving χ_c states are neglected and are accounted for in the systematic uncertainties.

The background processes $B_c^+ \rightarrow J/\psi H_c X$ are modeled using a cocktail of two-body decays and quasi-two-body decays that proceed through excited D_s^+ resonances. Several decay modes in the cocktail have recently been measured at LHCb [34], and for others the branching fractions are fixed by analogy to the well-measured $B \rightarrow D^* H_c X$ decays [29]. The cocktail consists of the two-body and quasi-two-body decays in equal proportion.

The decay-time distributions derived from simulated B_c^+ decays are corrected for acceptance differences between the data and simulation. This is achieved by applying weights to the simulated distribution from a study of a control sample of $J/\psi K^+$ combinations from the decay $B^0 \rightarrow J/\psi K^*(892)^0$ with $K^*(892)^0 \rightarrow K^+\pi^-$ in the data and simulation; the weights are calculated in bins of the decay time and of the relative momentum carried by the π^- omitted from the combination [analogous to that of the unobserved neutrino(s) in the simulation samples]. The B_c^+ lifetime is allowed to vary in the fit, constrained by its measured value and precision.

The combinatorial background in the selected $J/\psi\mu^+$ sample is predominantly due to J/ψ mesons from $B_{u,d,s} \rightarrow J/\psi X$ decays paired with muon candidates from the rest of the event. This background source is modeled using a set of three template histograms taken from simulation for the three B -meson species, with their relative fractions constrained in accordance with the production cross sections and their respective branching fractions. A fit is performed to the $J/\psi\mu^+$ mass distribution above $6.4 \text{ GeV}/c^2$, higher than the B_c^+ mass, to validate the modeling of this background and correct for possible sources of combinatorial background in the data unaccounted for by the model, including decays of b baryons and the effect of unknown branching fractions. A linear correction to the $J/\psi\mu^+$ mass distribution in the simulation is determined by this fit and applied to the combinatorial background templates, and it is varied within bounds to determine a systematic uncertainty.

A separate background comes from pairing unrelated muons to form J/ψ candidates. The template for this combinatorial J/ψ component is determined using events where the J/ψ invariant mass lies above the nominal selection threshold, with its normalization fixed using a fit to the $\mu^+\mu^-$ invariant-mass distribution. Two models for the shape of the combinatorial background in the J/ψ mass distribution are considered. The nominal fit uses a mixture of distributions with Gaussian cores and power law tails [35] for the true $J/\psi \rightarrow \mu^+\mu^-$ component and an exponential function for the combinatorial background. An alternative fit is performed to evaluate a corresponding systematic uncertainty.

The largest background component is due to the inclusive decays of light b hadrons to J/ψ mesons, in which an accompanying pion or kaon (or, less frequently, proton or electron) is misidentified as a muon, hereafter referred to as

the mis-ID background. A data-driven approach is used to construct templates for this background component. A sample of $J/\psi h^+$ candidates, where h^+ stands for a charged hadron, is selected following similar criteria to those of the signal sample but with the h^+ failing the muon identification criteria. This control sample is enriched in various hadron species (primarily, pions, kaons, and protons) and electrons. Using several high-purity control samples of identified hadrons, weights are computed that represent the probability that a hadron with particular kinematic properties would pass the muon criteria. These weights are applied to the $J/\psi h^+$ sample to generate binned templates representing these background components. The normalization of each of these components is allowed to vary in the fit to the data.

A binned maximum likelihood fit is performed using the templates representing the various components. The number of candidates from each component, with the exception of the combinatorial J/ψ background, are allowed to vary in the fit, as are the shape parameters corresponding to the B_c^+ lifetime and the $A_0(q^2)$ form factor. The contributions of the feed-down processes involving the decays of higher-mass charmonium states $B_c^+ \rightarrow \psi(2S)\mu^+\nu_\mu$, $B_c^+ \rightarrow \chi_{c(0,1,2)}(1P)\mu^+\nu_\mu$ are allowed to vary in the fit, whereas the ratio of the branching fractions $\mathcal{R}[\psi(2S)] = \mathcal{B}[B_c^+ \rightarrow \psi(2S)\tau^+\nu_\tau]/\mathcal{B}[B_c^+ \rightarrow \psi(2S)\mu^+\nu_\mu]$ is fixed to the predicted SM value of 8.5% [18]. This is later varied for the evaluation of a systematic uncertainty.

Extensive studies of the fit procedure are carried out to identify potential sources of bias in the fit. Simulated signal is added to the data histograms, and the resulting changes in the value of $\mathcal{R}(J/\psi)$ from the fit are found to be consistent with the injected signal increments. The procedure is also applied to the mis-ID background, which shows no bias in the fitted number of events as a function of injected events. Another important consideration for this measurement is the disparate properties of the various templates. Some templates are populated in all kinematically allowed bins, such as the mis-ID background that is derived from large data samples. Others are sparsely populated and contain empty bins, e.g., for modes with low efficiency and yields that are obtained from simulated events. Pseudoexperiments with template compositions similar to those in this analysis reveal a possible bias of the fit results. Hence, the binning scheme for this analysis is chosen to minimize the number of empty bins in the sparsely populated templates, while retaining the discriminating power of the distributions. Kernel density estimation (KDE) [36] is used to derive continuous distributions representative of the nominal fit templates. Simulated pseudoexperiments using histogram templates sampled from these continuous distributions are then used to evaluate any remaining bias that results. Based on these studies, a Bayesian procedure is implemented for correcting the raw $\mathcal{R}(J/\psi)$ value after unblinding.

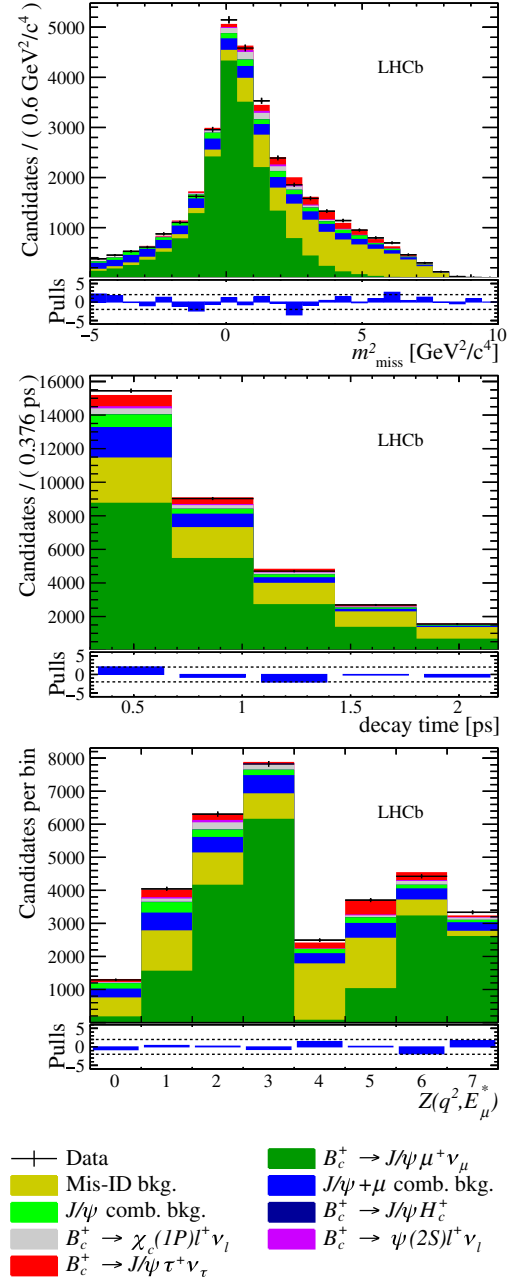


FIG. 1. Distributions of (top) m_{miss}^2 , (middle) decay time, and (bottom) Z of the signal data overlaid with projections of the fit model with all normalization and shape parameters at their best-fit values. Below each panel, differences between the data and fit are shown, normalized by the Poisson uncertainty in the data; the dashed lines are at the values ± 2 .

The results of the fit are presented in Fig. 1 showing the projections of the nominal fit result onto the quantities m_{miss}^2 , decay time, and Z . The fit yields 1400 ± 300 signal and 19140 ± 340 normalization decays, where the errors are statistical and correlated. Accounting for the $\tau^+ \rightarrow \mu^+\nu_\mu\bar{\nu}_\tau$ branching fraction and the ratio of efficiencies $[(52.4 \pm 0.4)\%]$ gives an uncorrected value of 0.79 for $\mathcal{R}(J/\psi)$. Correcting for the mean expected bias at this

value, we obtain $\mathcal{R}(J/\psi) = 0.71 \pm 0.17(\text{stat})$. The significance of the signal determined from a likelihood scan procedure and corrected for the systematic uncertainty is found to be 3 standard deviations.

Systematic uncertainties on $\mathcal{R}(J/\psi)$ are listed in Table I. The effect of the limited size of the toy simulated data on the template shapes is determined using the procedure of Refs. [37,38]. In the nominal fit, the $B_c^+ \rightarrow J/\psi$ form factor parameters, except for the scalar form factor that primarily affects the semitauonic mode, are fixed to the values obtained from a fit to a subset of the data enriched in the normalization mode. To assess the effect on $\mathcal{R}(J/\psi)$ due to this procedure, an alternative fit is performed with the form factor parameters allowed to vary, and the difference in quadrature of the uncertainties is assigned as a systematic uncertainty. The effect due to the $B_c^+ \rightarrow \psi(2S)$ form factors is evaluated by comparing fits using two different theoretical models for this template [18,31].

The systematic uncertainty of the bias correction is calculated from the difference in bias between fits to the simulated data based on a set of realistic parametrized distributions and corresponding fits based on KDE versions of these distributions. The effect of the placement of the bin thresholds in the quantity Z is determined by varying the boundaries of the thresholds in E_μ^* and q^2 and by reducing the number of bins in the fit. The data-driven method employed to determine the mis-ID background is repeated with an alternative approach for modeling the effect of misreconstructed tracks within the mis-ID control sample (rejected from the nominal sample by muon PID requirements). The fit procedure is repeated with templates derived from this alternative method, and an uncertainty is assigned using half the difference between the resulting central value of $\mathcal{R}(J/\psi)$ and the nominal value. The systematic uncertainty due to the combinatorial background model is determined by varying the linear correction made to its $J/\psi\mu^+$ mass distribution described above, within its bounds. The uncertainty due to the combinatorial background in the J/ψ peak region is determined by varying the normalization of this component within the range determined from the alternative fit to the invariant-mass distribution of J/ψ candidates.

The systematic uncertainty due to the contribution of the process $B_c^+ \rightarrow J/\psi H_c X$, which is poorly resolved by the fit, is determined by fixing the yield relative to the normalization to that expected from the estimated branching fraction for these decays [29,34]. The effect of fixing the contribution of the semitauonic decay $B_c^+ \rightarrow \psi(2S)\tau^+\nu_\mu$ is determined by varying $\mathcal{R}[\psi(2S)]$ by $\pm 50\%$ of the predicted value. The background from the feed-down decays $B_c^+ \rightarrow X(3872)\mu^+\nu_\mu$ with the principal decay chains $X(3872) \rightarrow J/\psi\pi^+\pi^-$ and $X(3872) \rightarrow J/\psi\gamma$ is kinematically similar to the background from $B_c^+ \rightarrow \psi(2S)\tau^+\nu_\mu$. An approximate bound on the number of $X(3872)$ candidates in the sample is obtained from the invariant mass distribution of $J/\psi\pi^+\pi^-$

TABLE I. Systematic uncertainties in the determination of $\mathcal{R}(J/\psi)$.

Source of uncertainty	Size ($\times 10^{-2}$)
Finite simulation size	8.0
$B_c^+ \rightarrow J/\psi$ form factors	12.1
$B_c^+ \rightarrow \psi(2S)$ form factors	3.2
Fit bias correction	5.4
Z binning strategy	5.6
Mis-ID background strategy	5.6
combinatorial background cocktail	4.5
combinatorial J/ψ background scaling	0.9
$B_c^+ \rightarrow J/\psi H_c X$ contribution	3.6
$\psi(2S)$ and χ_c feed-down	0.9
Weighting of simulation samples	1.6
Efficiency ratio	0.6
$\mathcal{B}(\tau^+ \rightarrow \mu^+\nu_\mu\bar{\nu}_\tau)$	0.2
Systematic uncertainty	17.7
Statistical uncertainty	17.3

combinations in the sample. This bound is found to be less than the uncertainty in the $\psi(2S)$ yield, and, thus, no additional uncertainty is assigned. In general, the effect of charmonium states above the open-charm threshold, which have large total width, are negligible as a result of their small decay rate to final states containing J/ψ . The uncertainty due to the small contribution of semitauonic decays involving χ_c states is assessed by assuming that the entire yield for this mode is absorbed in the signal mode and is summed in quadrature with that from the $\psi(2S)$ feed-down mode.

The systematic uncertainty due to the weighting of the simulation distributions of event parameters (the track multiplicity and the separation significances of the J/ψ and of the unpaired muon) is determined by varying the criteria for the definition of the subset of the data sample enriched in the normalization mode used in the weighting procedure and employing alternative methods to account for the misidentified muon candidates in the sample. The uncertainty in the efficiency ratio measured in simulation is propagated to $\mathcal{R}(J/\psi)$ and is dominated by the statistical uncertainty of the simulation sample.

In summary, the decay $B_c^+ \rightarrow J/\psi\tau^+\nu_\tau$ is studied using data corresponding to 3 fb^{-1} recorded with the LHCb detector during 2011 and 2012, leading to the first measurement of the ratio of branching fractions

$$\begin{aligned} \mathcal{R}(J/\psi) &= \frac{\mathcal{B}(B_c^+ \rightarrow J/\psi\tau^+\nu_\tau)}{\mathcal{B}(B_c^+ \rightarrow J/\psi\mu^+\nu_\mu)} \\ &= 0.71 \pm 0.17(\text{stat}) \pm 0.18(\text{syst}). \end{aligned} \quad (3)$$

This result lies within 2 standard deviations of the range of central values currently predicted by the standard model, 0.25–0.28.

We express our gratitude to our colleagues in the CERN accelerator departments for the excellent performance of the LHC. We thank the technical and administrative staff at the LHCb institutes. We acknowledge support from CERN and from the national agencies: CAPES, CNPq, FAPERJ, and FINEP (Brazil); MOST and NSFC (China); CNRS/IN2P3 (France); BMBF, DFG, and MPG (Germany); INFN (Italy); NWO (Netherlands); MNiSW and NCN (Poland); MEN/IFA (Romania); MinES and FASO (Russia); MinECo (Spain); SNSF and SER (Switzerland); NASU (Ukraine); STFC (United Kingdom); NSF (USA). We acknowledge the computing resources that are provided by CERN, IN2P3 (France), KIT and DESY (Germany), INFN (Italy), SURF (Netherlands), PIC (Spain), GridPP (United Kingdom), RRCKI and Yandex LLC (Russia), CSCS (Switzerland), IFIN-HH (Romania), CBPF (Brazil), PL-GRID (Poland), and OSC (USA). We are indebted to the communities behind the multiple open-source software packages on which we depend. Individual groups or members have received support from AvH Foundation (Germany), EPLANET, Marie Skłodowska-Curie Actions, and ERC (European Union), ANR, Labex P2IO, ENIGMASS, and OCEVU, and Région Auvergne-Rhône-Alpes (France), RFBR and Yandex LLC (Russia), GVA, XuntaGal, and GENCAT (Spain), Herchel Smith Fund, the Royal Society, the English-Speaking Union, and the Leverhulme Trust (United Kingdom).

-
- [1] J. P. Lees *et al.* (BABAR Collaboration), *Phys. Rev. Lett.* **109**, 101802 (2012).
- [2] J. P. Lees *et al.* (BABAR Collaboration), *Phys. Rev. D* **88**, 072012 (2013).
- [3] M. Huschle *et al.* (Belle Collaboration), *Phys. Rev. D* **92**, 072014 (2015).
- [4] Y. Sato *et al.* (Belle Collaboration), *Phys. Rev. D* **94**, 072007 (2016).
- [5] S. Hirose *et al.* (Belle Collaboration), *Phys. Rev. Lett.* **118**, 211801 (2017).
- [6] S. Hirose *et al.* (Belle Collaboration), arXiv:1709.00129.
- [7] R. Aaij *et al.* (LHCb Collaboration), *Phys. Rev. Lett.* **115**, 111803 (2015).
- [8] R. Aaij *et al.* (LHCb Collaboration), arXiv:1708.08856.
- [9] R. Aaij *et al.* (LHCb Collaboration), arXiv:1711.02505.
- [10] Y. Amhis *et al.* (Heavy Flavor Averaging Group), arXiv:1612.07233 [updated results and plots available at <http://www.slac.stanford.edu/xorg/hflav/>].
- [11] M. Tanaka, *Z. Phys. C* **67**, 321 (1995).
- [12] A. Crivellin, C. Greub, and A. Kokulu, *Phys. Rev. D* **86**, 054014 (2012).
- [13] M. Freytsis, Z. Ligeti, and J. T. Ruderman, *Phys. Rev. D* **92**, 054018 (2015).
- [14] A. Crivellin, G. D'Ambrosio, and J. Heeck, *Phys. Rev. D* **91**, 075006 (2015).
- [15] R. Aaij *et al.* (LHCb Collaboration), *Phys. Rev. Lett.* **113**, 151601 (2014).
- [16] R. Aaij *et al.* (LHCb Collaboration), *J. High Energy Phys.* **08** (2017) 055.
- [17] A. Yu. Anisimov, I. M. Narodetskii, C. Semay, and B. Silvestre-Brac, *Phys. Lett. B* **452**, 129 (1999).
- [18] V. Kiselev, arXiv:hep-ph/0211021.
- [19] M. A. Ivanov, J. G. Korner, and P. Santorelli, *Phys. Rev. D* **73**, 054024 (2006).
- [20] E. Hernández, J. Nieves, and J. M. Verde-Velasco, *Phys. Rev. D* **74**, 074008 (2006).
- [21] A. A. Alves, Jr. *et al.* (LHCb Collaboration), *J. Instrum.* **3**, S08005 (2008).
- [22] R. Aaij *et al.* (LHCb Collaboration), *Int. J. Mod. Phys. A* **30**, 1530022 (2015).
- [23] A. A. Alves, Jr. *et al.*, *J. Instrum.* **8**, P02022 (2013).
- [24] R. Aaij *et al.*, *J. Instrum.* **8**, P04022 (2013).
- [25] T. Sjöstrand, S. Mrenna, and P. Skands, *J. High Energy Phys.* **05** (2006) 026; *Comput. Phys. Commun.* **178**, 852 (2008).
- [26] I. Belyaev *et al.*, *J. Phys. Conf. Ser.* **331**, 032047 (2011).
- [27] C.-H. Chang, J.-X. Wang, and X.-G. Wu, *Comput. Phys. Commun.* **174**, 241 (2006).
- [28] J. Allison, K. Amako, J. Apostolakis, H. Araujo, P. Dubois *et al.* (Geant4 Collaboration), *IEEE Trans. Nucl. Sci.* **53**, 270 (2006); S. Agostinelli *et al.* (Geant4 Collaboration), *Nucl. Instrum. Methods Phys. Res., Sect. A* **506**, 250 (2003).
- [29] C. Patrignani *et al.* (Particle Data Group), *Chin. Phys. C* **40**, 100001 (2016), and 2017 update.
- [30] A. Rogozhnikov, *J. Phys. Conf. Ser.* **762**, 012036 (2016).
- [31] D. Ebert, R. N. Faustov, and V. O. Galkin, *Phys. Rev. D* **68**, 094020 (2003).
- [32] C. Bourrely, L. Lellouch, and I. Caprini, *Phys. Rev. D* **79**, 013008 (2009).
- [33] X. X. Wang, W. Wang, and C. D. Lü, *Phys. Rev. D* **79**, 114018 (2009).
- [34] R. Aaij *et al.* (LHCb Collaboration), *Phys. Rev. D* **87**, 112012 (2013).
- [35] T. Skwarnicki, Cracow, INP Report Nos. DESY-F31-86-02, DESY-F-31-86-02, 1986, <http://www-library.desy.de/cgi-bin/showprep.pl?DESY-F31-86-02>.
- [36] K. S. Cranmer, *Comput. Phys. Commun.* **136**, 198 (2001).
- [37] R. J. Barlow and C. Beeston, *Comput. Phys. Commun.* **77**, 219 (1993).
- [38] K. Cranmer, G. Lewis, L. Moneta, A. Shibata, and W. Verkerke (ROOT Collaboration), New York U. Report No. CERN-OPEN-2012-016, 2012, <https://cds.cern.ch/record/1456844>.

Correction: The copyright statement contained an error and has been corrected.

R. Aaij,⁴⁰ B. Adeva,³⁹ M. Adinolfi,⁴⁸ Z. Ajaltouni,⁵ S. Akar,⁵⁹ J. Albrecht,¹⁰ F. Alessio,⁴⁰ M. Alexander,⁵³
A. Alfonso Alberio,³⁸ S. Ali,⁴³ G. Alkhazov,³¹ P. Alvarez Cartelle,⁵⁵ A. A. Alves Jr,⁵⁹ S. Amato,² S. Amerio,²³ Y. Amhis,⁷
L. An,³ L. Anderlini,¹⁸ G. Andreassi,⁴¹ M. Andreotti,^{17,a} J. E. Andrews,⁶⁰ R. B. Appleby,⁵⁶ F. Archilli,⁴³ P. d'Argent,¹²
J. Arnau Romeu,⁶ A. Artamonov,³⁷ M. Artuso,⁶¹ E. Aslanides,⁶ M. Atzeni,⁴² G. Auriemma,²⁶ M. Baalouch,⁵
I. Babuschkin,⁵⁶ S. Bachmann,¹² J. J. Back,⁵⁰ A. Badalov,^{38,b} C. Baesso,⁶² S. Baker,⁵⁵ V. Balagura,^{7,c} W. Baldini,¹⁷
A. Baranov,³⁵ R. J. Barlow,⁵⁶ C. Barschel,⁴⁰ S. Barsuk,⁷ W. Barter,⁵⁶ F. Baryshnikov,³² V. Batozskaya,²⁹ V. Battista,⁴¹
A. Bay,⁴¹ L. Beaucourt,⁴ J. Beddow,⁵³ F. Bedeschi,²⁴ I. Bediaga,¹ A. Beiter,⁶¹ L. J. Bel,⁴³ N. Belyi,⁶³ V. Bellee,⁴¹
N. Belloli,^{21,d} K. Belous,³⁷ I. Belyaev,^{32,40} E. Ben-Haim,⁸ G. Bencivenni,¹⁹ S. Benson,⁴³ S. Beranek,⁹ A. Berezhnoy,³³
R. Bernet,⁴² D. Berninghoff,¹² E. Bertholet,⁸ A. Bertolin,²³ C. Betancourt,⁴² F. Betti,¹⁵ M.-O. Bettler,⁴⁰ M. van Beuzekom,⁴³
Ia. Bezshyiko,⁴² S. Bifani,⁴⁷ P. Billoir,⁸ A. Birnkraut,¹⁰ A. Bizzeti,^{18,e} M. Bjørn,⁵⁷ T. Blake,⁵⁰ F. Blanc,⁴¹ S. Blusk,⁶¹
V. Bocci,²⁶ T. Boettcher,⁵⁸ A. Bondar,^{36,f} N. Bondar,³¹ I. Bordyuzhin,³² S. Borghi,⁵⁶ M. Borisyak,³⁵ M. Borsato,³⁹ F. Bossu,⁷
M. Boubdir,⁹ T. J. V. Bowcock,⁵⁴ E. Bowen,⁴² C. Bozzi,^{17,40} S. Braun,¹² T. Britton,⁶¹ J. Brodzicka,²⁷ D. Brundu,¹⁶
E. Buchanan,⁴⁸ C. Burr,⁵⁶ A. Bursche,^{16,g} J. Buytaert,⁴⁰ W. Byczynski,⁴⁰ S. Cadeddu,¹⁶ H. Cai,⁶⁴ R. Calabrese,^{17,a}
R. Calladine,⁴⁷ M. Calvi,^{21,d} M. Calvo Gomez,^{38,b} A. Camboni,^{38,b} P. Campana,¹⁹ D. H. Campora Perez,⁴⁰ L. Capriotti,⁵⁶
A. Carbone,^{15,h} G. Carboni,^{25,i} R. Cardinale,^{20,j} A. Cardini,¹⁶ P. Carniti,^{21,d} L. Carson,⁵² K. Carvalho Akiba,² G. Casse,⁵⁴
L. Cassina,²¹ M. Cattaneo,⁴⁰ G. Cavallero,^{20,40,j} R. Cenci,^{24,k} D. Chamont,⁷ M. G. Chapman,⁴⁸ M. Charles,⁸
Ph. Charpentier,⁴⁰ G. Chatzikonstantinidis,⁴⁷ M. Chefdeville,⁴ S. Chen,¹⁶ S. F. Cheung,⁵⁷ S.-G. Chitic,⁴⁰ V. Chobanova,^{39,40}
M. Chrzascz,^{42,27} A. Chubykin,³¹ P. Ciambrone,¹⁹ X. Cid Vidal,³⁹ G. Ciezarek,⁴³ P. E. L. Clarke,⁵² M. Clemencic,⁴⁰
H. V. Cliff,⁴⁹ J. Closier,⁴⁰ J. Cogan,⁶ E. Cogneras,⁵ V. Cogoni,^{16,g} L. Cojocariu,³⁰ P. Collins,⁴⁰ T. Colombo,⁴⁰
A. Comerma-Montells,¹² A. Contu,⁴⁰ A. Cook,⁴⁸ G. Coombs,⁴⁰ S. Coquereau,³⁸ G. Corti,⁴⁰ M. Corvo,^{17,a}
C. M. Costa Sobral,⁵⁰ B. Couturier,⁴⁰ G. A. Cowan,⁵² D. C. Craik,⁵⁸ A. Crocombe,⁵⁰ M. Cruz Torres,¹ R. Currie,⁵²
C. D'Ambrosio,⁴⁰ F. Da Cunha Marinho,² E. Dall'Occo,⁴³ J. Dalseno,⁴⁸ A. Davis,³ O. De Aguiar Francisco,⁴⁰
K. De Bruyn,⁴⁰ S. De Capua,⁵⁶ M. De Cian,¹² J. M. De Miranda,¹ L. De Paula,² M. De Serio,^{14,l} P. De Simone,¹⁹
C. T. Dean,⁵³ D. Decamp,⁴ L. Del Buono,⁸ H.-P. Dembinski,¹¹ M. Demmer,¹⁰ A. Dendek,²⁸ D. Derkach,³⁵ O. Deschamps,⁵
F. Dettori,⁵⁴ B. Dey,⁶⁵ A. Di Canto,⁴⁰ P. Di Nezza,¹⁹ H. Dijkstra,⁴⁰ F. Dordei,⁴⁰ M. Dorigo,⁴⁰ A. Dosil Suárez,³⁹ L. Douglas,⁵³
A. Dovbnya,⁴⁵ K. Dreimanis,⁵⁴ L. Dufour,⁴³ G. Dujany,⁸ P. Durante,⁴⁰ R. Dzhelyadin,³⁷ M. Dziewiecki,¹² A. Dziurda,⁴⁰
A. Dzyuba,³¹ S. Easo,⁵¹ M. Ebert,⁵² U. Egede,⁵⁵ V. Egorychev,³² S. Eidelman,^{36,f} S. Eisenhardt,⁵² U. Eitschberger,¹⁰
R. Ekelhof,¹⁰ L. Eklund,⁵³ S. Ely,⁶¹ S. Esen,¹² H. M. Evans,⁴⁹ T. Evans,⁵⁷ A. Falabella,¹⁵ N. Farley,⁴⁷ S. Farry,⁵⁴
D. Fazzini,^{21,d} L. Federici,²⁵ D. Ferguson,⁵² G. Fernandez,³⁸ P. Fernandez Declara,⁴⁰ A. Fernandez Prieto,³⁹ F. Ferrari,¹⁵
F. Ferreira Rodrigues,² M. Ferro-Luzzi,⁴⁰ S. Filippov,³⁴ R. A. Fini,¹⁴ M. Fiorini,^{17,a} M. Firlej,²⁸ C. Fitzpatrick,⁴¹
T. Fiutowski,²⁸ F. Fleuret,^{7,c} K. Fohl,⁴⁰ M. Fontana,^{16,40} F. Fontanelli,^{20,j} D. C. Forshaw,⁶¹ R. Forty,⁴⁰ V. Franco Lima,⁵⁴
M. Frank,⁴⁰ C. Frei,⁴⁰ J. Fu,^{22,m} W. Funk,⁴⁰ E. Furfaro,^{25,i} C. Färber,⁴⁰ E. Gabriel,⁵² A. Gallas Torreira,³⁹ D. Galli,^{15,h}
S. Gallorini,²³ S. Gambetta,⁵² M. Gandelman,² P. Gandini,²² Y. Gao,³ L. M. Garcia Martin,⁷⁰ J. García Pardiñas,³⁹
J. Garra Tico,⁴⁹ L. Garrido,³⁸ P. J. Garsed,⁴⁹ D. Gascon,³⁸ C. Gaspar,⁴⁰ L. Gavardi,¹⁰ G. Gazzoni,⁵ D. Gerick,¹²
E. Gersabeck,⁵⁶ M. Gersabeck,⁵⁶ T. Gershon,⁵⁰ Ph. Ghez,⁴ S. Gianì,⁴¹ V. Gibson,⁴⁹ O. G. Girard,⁴¹ L. Giubega,³⁰
K. Gizdov,⁵² V. V. Gligorov,⁸ D. Golubkov,³² A. Golutvin,⁵⁵ A. Gomes,^{1,n} I. V. Gorelov,³³ C. Gotti,^{21,d} E. Govorkova,⁴³
J. P. Grabowski,¹² R. Graciani Diaz,³⁸ L. A. Granado Cardoso,⁴⁰ E. Graugés,³⁸ E. Graverini,⁴² G. Graziani,¹⁸ A. Greco,³⁰
R. Greim,⁹ P. Griffith,¹⁶ L. Grillo,²¹ L. Gruber,⁴⁰ B. R. Gruber Cazon,⁵⁷ O. Grünberg,⁶⁷ E. Gushchin,³⁴ Yu. Guz,³⁷ T. Gys,⁴⁰
C. Göbel,⁶² T. Hadavizadeh,⁵⁷ C. Hadjivasiliou,⁵ G. Haefeli,⁴¹ C. Haen,⁴⁰ S. C. Haines,⁴⁹ B. Hamilton,⁶⁰ X. Han,¹²
T. H. Hancock,⁵⁷ S. Hansmann-Menzemer,¹² N. Harnew,⁵⁷ S. T. Harnew,⁴⁸ C. Hasse,⁴⁰ M. Hatch,⁴⁰ J. He,⁶³ M. Hecker,⁵⁵
K. Heinicke,¹⁰ A. Heister,⁹ K. Hennessy,⁵⁴ P. Henrard,⁵ L. Henry,⁷⁰ E. van Herwijnen,⁴⁰ M. Heß,⁶⁷ A. Hicheur,² D. Hill,⁵⁷
C. Hombach,⁵⁶ P. H. Hopchev,⁴¹ W. Hu,⁶⁵ Z. C. Huard,⁵⁹ W. Hulsbergen,⁴³ T. Humair,⁵⁵ M. Hushchyn,³⁵ D. Hutchcroft,⁵⁴
P. Ibis,¹⁰ M. Idzik,²⁸ P. Ilten,⁵⁸ R. Jacobsson,⁴⁰ J. Jalocha,⁵⁷ E. Jans,⁴³ A. Jawahery,⁶⁰ F. Jiang,³ M. John,⁵⁷ D. Johnson,⁴⁰
C. R. Jones,⁴⁹ C. Joram,⁴⁰ B. Jost,⁴⁰ N. Jurik,⁵⁷ S. Kandybei,⁴⁵ M. Karacson,⁴⁰ J. M. Kariuki,⁴⁸ S. Karodia,⁵³ N. Kazeev,³⁵
M. Kecke,¹² F. Keizer,⁴⁹ M. Kelsey,⁶¹ M. Kenzie,⁴⁹ T. Ketel,⁴⁴ E. Khairullin,³⁵ B. Khanji,¹² C. Khurewathanakul,⁴¹ T. Kirn,⁹
S. Klaver,⁵⁶ K. Klimaszewski,²⁹ T. Klimkovich,¹¹ S. Koliiev,⁴⁶ M. Kolpin,¹² R. Kopecna,¹² P. Koppenburg,⁴³
A. Kosmyntseva,³² S. Kotriakhova,³¹ M. Kozeiha,⁵ L. Kravchuk,³⁴ M. Kreps,⁵⁰ F. Kress,⁵⁵ P. Krokovny,^{36,f} F. Kruse,¹⁰
W. Krzemien,²⁹ W. Kucewicz,^{27,o} M. Kucharczyk,²⁷ V. Kudryavtsev,^{36,f} A. K. Kuonen,⁴¹ T. Kvaratskheliya,^{32,40}
D. Lacarrere,⁴⁰ G. Lafferty,⁵⁶ A. Lai,¹⁶ G. Lanfranchi,¹⁹ C. Langenbruch,⁹ T. Latham,⁵⁰ C. Lazzeroni,⁴⁷ R. Le Gac,⁶

A. Leflat,^{33,40} J. Lefrançois,⁷ R. Lefèvre,⁵ F. Lemaitre,⁴⁰ E. Lemos Cid,³⁹ O. Leroy,⁶ T. Lesiak,²⁷ B. Leverington,¹² P.-R. Li,⁶³ T. Li,³ Y. Li,⁷ Z. Li,⁶¹ T. Likhomanenko,⁶⁸ R. Lindner,⁴⁰ F. Lionetto,⁴² V. Lisovskyi,⁷ X. Liu,³ D. Loh,⁵⁰ A. Loi,¹⁶ I. Longstaff,⁵³ J. H. Lopes,² D. Lucchesi,^{23,p} M. Lucio Martinez,³⁹ H. Luo,⁵² A. Lupato,²³ E. Luppi,^{17,a} O. Lupton,⁴⁰ A. Lusiani,²⁴ X. Lyu,⁶³ F. Machefert,⁷ F. Maciuc,³⁰ V. Macko,⁴¹ P. Mackowiak,¹⁰ S. Maddrell-Mander,⁴⁸ O. Maev,^{31,40} K. Maguire,⁵⁶ D. Maisuzenko,³¹ M. W. Majewski,²⁸ S. Malde,⁵⁷ B. Malecki,²⁷ A. Malinin,⁶⁸ T. Maltsev,^{36,f} G. Manca,^{16,g} G. Mancinelli,⁶ D. Marangotto,^{22,m} J. Maratas,^{5,q} J. F. Marchand,⁴ U. Marconi,¹⁵ C. Marin Benito,³⁸ M. Marinangeli,⁴¹ P. Marino,⁴¹ J. Marks,¹² G. Martellotti,²⁶ M. Martin,⁶ M. Martinelli,⁴¹ D. Martinez Santos,³⁹ F. Martinez Vidal,⁷⁰ L. M. Massacrier,⁷ A. Massafferri,¹ R. Matev,⁴⁰ A. Mathad,⁵⁰ Z. Mathe,⁴⁰ C. Matteuzzi,²¹ A. Mauri,⁴² E. Maurice,^{7,c} B. Maurin,⁴¹ A. Mazurov,⁴⁷ M. McCann,^{55,40} A. McNab,⁵⁶ R. McNulty,¹³ J. V. Mead,⁵⁴ B. Meadows,⁵⁹ C. Meaux,⁶ F. Meier,¹⁰ N. Meinert,⁶⁷ D. Melnychuk,²⁹ M. Merk,⁴³ A. Merli,^{22,40,m} E. Michielin,²³ D. A. Milanese,⁶⁶ E. Millard,⁵⁰ M.-N. Minard,⁴ L. Minzoni,¹⁷ D. S. Mitzel,¹² A. Mogini,⁸ J. Molina Rodriguez,¹ T. Mombächer,¹⁰ I. A. Monroy,⁶⁶ S. Monteil,⁵ M. Morandin,²³ M. J. Morello,^{24,k} O. Morgunova,⁶⁸ J. Moron,²⁸ A. B. Morris,⁵² R. Mountain,⁶¹ F. Muheim,⁵² M. Mulder,⁴³ D. Müller,⁵⁶ J. Müller,¹⁰ K. Müller,⁴² V. Müller,¹⁰ P. Naik,⁴⁸ T. Nakada,⁴¹ R. Nandakumar,⁵¹ A. Nandi,⁵⁷ I. Nasteva,² M. Needham,⁵² N. Neri,^{22,40} S. Neubert,¹² N. Neufeld,⁴⁰ M. Neuner,¹² T. D. Nguyen,⁴¹ C. Nguyen-Mau,^{41,r} S. Nieswand,⁹ R. Niet,¹⁰ N. Nikitin,³³ T. Nikodem,¹² A. Nogay,⁶⁸ D. P. O'Hanlon,⁵⁰ A. Oblakowska-Mucha,²⁸ V. Obraztsov,³⁷ S. Ogilvy,¹⁹ R. Oldeman,^{16,g} C. J. G. Onderwater,⁷¹ A. Ossowska,²⁷ J. M. Otorola Goicochea,² P. Owen,⁴² A. Oyanguren,⁷⁰ P. R. Pais,⁴¹ A. Palano,¹⁴ M. Palutan,^{19,40} A. Papanestis,⁵¹ M. Pappagallo,^{14,l} L. L. Pappalardo,^{17,a} W. Parker,⁶⁰ C. Parkes,⁵⁶ G. Passaleva,^{18,40} A. Pastore,^{14,l} M. Patel,⁵⁵ C. Patrignani,^{15,h} A. Pearce,⁴⁰ A. Pellegrino,⁴³ G. Penso,²⁶ M. Pepe Altarelli,⁴⁰ S. Perazzini,⁴⁰ P. Perret,⁵ L. Pescatore,⁴¹ K. Petridis,⁴⁸ A. Petrolini,^{20,j} A. Petrov,⁶⁸ M. Petruzzo,^{22,m} E. Picatoste Olloqui,³⁸ B. Pietrzyk,⁴ M. Pikies,²⁷ D. Pinci,²⁶ F. Pisani,⁴⁰ A. Pistone,^{20,j} A. Piucci,¹² V. Placinta,³⁰ S. Playfer,⁵² M. Plo Casasus,³⁹ F. Polci,⁸ M. Poli Lener,¹⁹ A. Poluektov,⁵⁰ I. Polyakov,⁶¹ E. Polycarpo,² G. J. Pomery,⁴⁸ S. Ponce,⁴⁰ A. Popov,³⁷ D. Popov,^{11,40} S. Poslavskii,³⁷ C. Potterat,² E. Price,⁴⁸ J. Prisciandaro,³⁹ C. Prouve,⁴⁸ V. Pugatch,⁴⁶ A. Puig Navarro,⁴² H. Pullen,⁵⁷ G. Punzi,^{24,s} W. Qian,⁵⁰ R. Quagliani,^{7,48} B. Quintana,⁵ B. Rachwal,²⁸ J. H. Rademacker,⁴⁸ M. Rama,²⁴ M. Ramos Pernas,³⁹ M. S. Rangel,² I. Raniuk,^{45,†} F. Ratnikov,³⁵ G. Raven,⁴⁴ M. Ravonel Salzgeber,⁴⁰ M. Reboud,⁴ F. Redi,⁵⁵ S. Reichert,¹⁰ A. C. dos Reis,¹ C. Remon Alepuz,⁷⁰ V. Renaudin,⁷ S. Ricciardi,⁵¹ S. Richards,⁴⁸ M. Rihl,⁴⁰ K. Rinnert,⁵⁴ V. Rives Molina,³⁸ P. Robbe,⁷ A. Robert,⁸ A. B. Rodrigues,¹ E. Rodrigues,⁵⁹ J. A. Rodriguez Lopez,⁶⁶ A. Rogozhnikov,³⁵ S. Roiser,⁴⁰ A. Rollings,⁵⁷ V. Romanovskiy,³⁷ A. Romero Vidal,³⁹ J. W. Ronayne,¹³ M. Rotondo,¹⁹ M. S. Rudolph,⁶¹ T. Ruf,⁴⁰ P. Ruiz Valls,⁷⁰ J. Ruiz Vidal,⁷⁰ J. J. Saborido Silva,³⁹ E. Sadykhov,³² N. Sagidova,³¹ B. Saitta,^{16,g} V. Salustino Guimaraes,⁶² C. Sanchez Mayordomo,⁷⁰ B. Sanmartin Sedes,³⁹ R. Santacesaria,²⁶ C. Santamarina Rios,³⁹ M. Santimaria,¹⁹ E. Santovetti,^{25,i} G. Sarpis,⁵⁶ A. Sarti,^{19,t} C. Satriano,^{26,u} A. Satta,²⁵ D. M. Saunders,⁴⁸ D. Savrina,^{32,33} S. Schael,⁹ M. Schellenberg,¹⁰ M. Schiller,⁵³ H. Schindler,⁴⁰ M. Schmelling,¹¹ T. Schmelzer,¹⁰ B. Schmidt,⁴⁰ O. Schneider,⁴¹ A. Schopper,⁴⁰ H. F. Schreiner,⁵⁹ M. Schubiger,⁴¹ M.-H. Schune,⁷ R. Schwemmer,⁴⁰ B. Sciascia,¹⁹ A. Sciubba,^{26,t} A. Semennikov,³² E. S. Sepulveda,⁸ A. Sergi,⁴⁷ N. Serra,⁴² J. Serrano,⁶ L. Sestini,²³ P. Seyfert,⁴⁰ M. Shapkin,³⁷ I. Shapoval,⁴⁵ Y. Shcheglov,³¹ T. Shears,⁵⁴ L. Shekhtman,^{36,f} V. Shevchenko,⁶⁸ B. G. Siddi,¹⁷ R. Silva Coutinho,⁴² L. Silva de Oliveira,² G. Simi,^{23,p} S. Simone,^{14,l} M. Sirendi,⁴⁹ N. Skidmore,⁴⁸ T. Skwarnicki,⁶¹ E. Smith,⁵⁵ I. T. Smith,⁵² J. Smith,⁴⁹ M. Smith,⁵⁵ I. Soares Lavra,¹ M. D. Sokoloff,⁵⁹ F. J. P. Soler,⁵³ B. Souza De Paula,² B. Spaan,¹⁰ P. Spradlin,⁵³ S. Sridharan,⁴⁰ F. Stagni,⁴⁰ M. Stahl,¹² S. Stahl,⁴⁰ P. Stefkó,⁴¹ S. Stefkova,⁵⁵ O. Steinkamp,⁴² S. Stemmler,¹² O. Stenyakin,³⁷ M. Stepanova,³¹ H. Stevens,¹⁰ S. Stone,⁶¹ B. Storaci,⁴² S. Stracka,^{24,s} M. E. Stramaglia,⁴¹ M. Straticiu,³⁰ U. Straumann,⁴² J. Sun,³ L. Sun,⁶⁴ W. Sutcliffe,⁵⁵ K. Swientek,²⁸ V. Syropoulos,⁴⁴ T. Szumlak,²⁸ M. Szymanski,⁶³ S. T'Jampens,⁴ A. Tayduganov,⁶ T. Tekampe,¹⁰ G. Tellarini,^{17,a} F. Teubert,⁴⁰ E. Thomas,⁴⁰ J. van Tilburg,⁴³ M. J. Tilley,⁵⁵ V. Tisserand,⁴ M. Tobin,⁴¹ S. Tolk,⁴⁹ L. Tomassetti,^{17,a} D. Tonelli,²⁴ F. Toriello,⁶¹ R. Tourinho Jadallah Aoude,¹ E. Tournefier,⁴ M. Traill,⁵³ M. T. Tran,⁴¹ M. Tresch,⁴² A. Trisovic,⁴⁰ A. Tsaregorodtsev,⁶ P. Tsopelas,⁴³ A. Tully,⁴⁹ N. Tuning,^{43,40} A. Ukleja,²⁹ A. Usachov,⁷ A. Ustyuzhanin,³⁵ U. Uwer,¹² C. Vacca,^{16,g} A. Vagner,⁶⁹ V. Vagnoni,^{15,40} A. Valassi,⁴⁰ S. Valat,⁴⁰ G. Valenti,¹⁵ R. Vazquez Gomez,⁴⁰ P. Vazquez Regueiro,³⁹ S. Vecchi,¹⁷ M. van Veghel,⁴³ J. J. Velthuis,⁴⁸ M. Veltri,^{18,v} G. Veneziano,⁵⁷ A. Venkateswaran,⁶¹ T. A. Verlage,⁹ M. Vernet,⁵ M. Vesterinen,⁵⁷ J. V. Viana Barbosa,⁴⁰ B. Viaud,⁷ D. Vieira,⁶³ M. Vieites Diaz,³⁹ H. Viemann,⁶⁷ X. Vilasis-Cardona,^{38,b} M. Vitti,⁴⁹ V. Volkov,³³ A. Vollhardt,⁴² B. Voneki,⁴⁰ A. Vorobyev,³¹ V. Vorobyev,^{36,f} C. Voß,⁹ J. A. de Vries,⁴³ C. Vázquez Sierra,³⁹ R. Waldi,⁶⁷ C. Wallace,⁵⁰ R. Wallace,¹³ J. Walsh,²⁴ J. Wang,⁶¹ D. R. Ward,⁴⁹

H. M. Wark,⁵⁴ N. K. Watson,⁴⁷ D. Websdale,⁵⁵ A. Weiden,⁴² C. Weisser,⁵⁸ M. Whitehead,⁴⁰ J. Wicht,⁵⁰ G. Wilkinson,⁵⁷ M. Wilkinson,⁶¹ M. Williams,⁵⁶ M. P. Williams,⁴⁷ M. Williams,⁵⁸ T. Williams,⁴⁷ F. F. Wilson,^{51,40} J. Wimberley,⁶⁰ M. Winn,⁷ J. Wishahi,¹⁰ W. Wislicki,²⁹ M. Witek,²⁷ G. Wormser,⁷ S. A. Wotton,⁴⁹ K. Wraight,⁵³ K. Wyllie,⁴⁰ Y. Xie,⁶⁵ M. Xu,⁶⁵ Z. Xu,⁴ Z. Yang,³ Z. Yang,⁶⁰ Y. Yao,⁶¹ H. Yin,⁶⁵ J. Yu,⁶⁵ X. Yuan,⁶¹ O. Yushchenko,³⁷ K. A. Zarebski,⁴⁷ M. Zavertyaev,^{11,w} L. Zhang,³ Y. Zhang,⁷ A. Zhelezov,¹² Y. Zheng,⁶³ X. Zhu,³ V. Zhukov,³³ J. B. Zonneveld,⁵² and S. Zucchelli¹⁵

(LHCb Collaboration)

- ¹*Centro Brasileiro de Pesquisas Físicas (CBPF), Rio de Janeiro, Brazil*
²*Universidade Federal do Rio de Janeiro (UFRJ), Rio de Janeiro, Brazil*
³*Center for High Energy Physics, Tsinghua University, Beijing, China*
⁴*LAPP, Université Savoie Mont-Blanc, CNRS/IN2P3, Annecy-Le-Vieux, France*
⁵*Clermont Université, Université Blaise Pascal, CNRS/IN2P3, LPC, Clermont-Ferrand, France*
⁶*Aix Marseille Univ, CNRS/IN2P3, CPPM, Marseille, France*
⁷*LAL, Univ. Paris-Sud, CNRS/IN2P3, Université Paris-Saclay, Orsay, France*
⁸*LPNHE, Université Pierre et Marie Curie, Université Paris Diderot, CNRS/IN2P3, Paris, France*
⁹*I. Physikalisches Institut, RWTH Aachen University, Aachen, Germany*
¹⁰*Fakultät Physik, Technische Universität Dortmund, Dortmund, Germany*
¹¹*Max-Planck-Institut für Kernphysik (MPIK), Heidelberg, Germany*
¹²*Physikalisches Institut, Ruprecht-Karls-Universität Heidelberg, Heidelberg, Germany*
¹³*School of Physics, University College Dublin, Dublin, Ireland*
¹⁴*Sezione INFN di Bari, Bari, Italy*
¹⁵*Sezione INFN di Bologna, Bologna, Italy*
¹⁶*Sezione INFN di Cagliari, Cagliari, Italy*
¹⁷*Università e INFN, Ferrara, Ferrara, Italy*
¹⁸*Sezione INFN di Firenze, Firenze, Italy*
¹⁹*Laboratori Nazionali dell'INFN di Frascati, Frascati, Italy*
²⁰*Sezione INFN di Genova, Genova, Italy*
²¹*Università e INFN, Milano-Bicocca, Milano, Italy*
²²*Sezione di Milano, Milano, Italy*
²³*Sezione INFN di Padova, Padova, Italy*
²⁴*Sezione INFN di Pisa, Pisa, Italy*
²⁵*Sezione INFN di Roma Tor Vergata, Roma, Italy*
²⁶*Sezione INFN di Roma La Sapienza, Roma, Italy*
²⁷*Henryk Niewodniczanski Institute of Nuclear Physics Polish Academy of Sciences, Kraków, Poland*
²⁸*AGH—University of Science and Technology, Faculty of Physics and Applied Computer Science, Kraków, Poland*
²⁹*National Center for Nuclear Research (NCBJ), Warsaw, Poland*
³⁰*Horia Hulubei National Institute of Physics and Nuclear Engineering, Bucharest-Magurele, Romania*
³¹*Petersburg Nuclear Physics Institute (PNPI), Gatchina, Russia*
³²*Institute of Theoretical and Experimental Physics (ITEP), Moscow, Russia*
³³*Institute of Nuclear Physics, Moscow State University (SINP MSU), Moscow, Russia*
³⁴*Institute for Nuclear Research of the Russian Academy of Sciences (INR RAN), Moscow, Russia*
³⁵*Yandex School of Data Analysis, Moscow, Russia*
³⁶*Budker Institute of Nuclear Physics (SB RAS), Novosibirsk, Russia*
³⁷*Institute for High Energy Physics (IHEP), Protvino, Russia*
³⁸*ICCUB, Universitat de Barcelona, Barcelona, Spain*
³⁹*Universidad de Santiago de Compostela, Santiago de Compostela, Spain*
⁴⁰*European Organization for Nuclear Research (CERN), Geneva, Switzerland*
⁴¹*Institute of Physics, Ecole Polytechnique Fédérale de Lausanne (EPFL), Lausanne, Switzerland*
⁴²*Physik-Institut, Universität Zürich, Zürich, Switzerland*
⁴³*Nikhef National Institute for Subatomic Physics, Amsterdam, Netherlands*
⁴⁴*Nikhef National Institute for Subatomic Physics and VU University Amsterdam, Amsterdam, Netherlands*
⁴⁵*NSC Kharkiv Institute of Physics and Technology (NSC KIPT), Kharkiv, Ukraine*
⁴⁶*Institute for Nuclear Research of the National Academy of Sciences (KINR), Kyiv, Ukraine*
⁴⁷*University of Birmingham, Birmingham, United Kingdom*
⁴⁸*H.H. Wills Physics Laboratory, University of Bristol, Bristol, United Kingdom*
⁴⁹*Cavendish Laboratory, University of Cambridge, Cambridge, United Kingdom*

- ⁵⁰*Department of Physics, University of Warwick, Coventry, United Kingdom*
⁵¹*STFC Rutherford Appleton Laboratory, Didcot, United Kingdom*
⁵²*School of Physics and Astronomy, University of Edinburgh, Edinburgh, United Kingdom*
⁵³*School of Physics and Astronomy, University of Glasgow, Glasgow, United Kingdom*
⁵⁴*Oliver Lodge Laboratory, University of Liverpool, Liverpool, United Kingdom*
⁵⁵*Imperial College London, London, United Kingdom*
⁵⁶*School of Physics and Astronomy, University of Manchester, Manchester, United Kingdom*
⁵⁷*Department of Physics, University of Oxford, Oxford, United Kingdom*
⁵⁸*Massachusetts Institute of Technology, Cambridge, Massachusetts, USA*
⁵⁹*University of Cincinnati, Cincinnati, Ohio, USA*
⁶⁰*University of Maryland, College Park, Maryland, USA*
⁶¹*Syracuse University, Syracuse, New York, USA*
⁶²*Pontifícia Universidade Católica do Rio de Janeiro (PUC-Rio), Rio de Janeiro, Brazil*
(associated with Universidade Federal do Rio de Janeiro (UFRJ), Rio de Janeiro, Brazil)
⁶³*University of Chinese Academy of Sciences, Beijing, China*
(associated with Center for High Energy Physics, Tsinghua University, Beijing, China)
⁶⁴*School of Physics and Technology, Wuhan University, Wuhan, China*
(associated with Center for High Energy Physics, Tsinghua University, Beijing, China)
⁶⁵*Institute of Particle Physics, Central China Normal University, Wuhan, Hubei, China*
(associated with Center for High Energy Physics, Tsinghua University, Beijing, China)
⁶⁶*Departamento de Física, Universidad Nacional de Colombia, Bogota, Colombia*
(associated with LPNHE, Université Pierre et Marie Curie, Université Paris Diderot, CNRS/IN2P3, Paris, France)
⁶⁷*Institut für Physik, Universität Rostock, Rostock, Germany*
(associated with Physikalisches Institut, Ruprecht-Karls-Universität Heidelberg, Heidelberg, Germany)
⁶⁸*National Research Centre Kurchatov Institute, Moscow, Russia*
(associated with Institute of Theoretical and Experimental Physics (ITEP), Moscow, Russia)
⁶⁹*National Research Tomsk Polytechnic University, Tomsk, Russia*
(associated with Institute of Theoretical and Experimental Physics (ITEP), Moscow, Russia)
⁷⁰*Instituto de Física Corpuscular, Centro Mixto Universidad de Valencia—CSIC, Valencia, Spain*
(associated with ICCUB, Universitat de Barcelona, Barcelona, Spain)
⁷¹*Van Swinderen Institute, University of Groningen, Groningen, Netherlands*
(associated with Nikhef National Institute for Subatomic Physics, Amsterdam, Netherlands)

[†]Deceased.

^aAlso at Università di Ferrara, Ferrara, Italy.

^bAlso at LIFAELS, La Salle, Universitat Ramon Llull, Barcelona, Spain.

^cAlso at Laboratoire Leprince-Ringuet, Palaiseau, France.

^dAlso at Università di Milano Bicocca, Milano, Italy.

^eAlso at Università di Modena e Reggio Emilia, Modena, Italy.

^fAlso at Novosibirsk State University, Novosibirsk, Russia.

^gAlso at Università di Cagliari, Cagliari, Italy.

^hAlso at Università di Bologna, Bologna, Italy.

ⁱAlso at Università di Roma Tor Vergata, Roma, Italy.

^jAlso at Università di Genova, Genova, Italy.

^kAlso at Scuola Normale Superiore, Pisa, Italy.

^lAlso at Università di Bari, Bari, Italy.

^mAlso at Università degli Studi di Milano, Milano, Italy.

ⁿAlso at Universidade Federal do Triângulo Mineiro (UFTM), Uberaba-MG, Brazil.

^oAlso at AGH—University of Science and Technology, Faculty of Computer Science, Electronics and Telecommunications, Kraków, Poland.

^pAlso at Università di Padova, Padova, Italy.

^qAlso at Iligan Institute of Technology (IIT), Iligan, Philippines.

^rAlso at Hanoi University of Science, Hanoi, Vietnam.

^sAlso at Università di Pisa, Pisa, Italy.

^tAlso at Università di Roma La Sapienza, Roma, Italy.

^uAlso at Università della Basilicata, Potenza, Italy.

^vAlso at Università di Urbino, Urbino, Italy.

^wAlso at P. N. Lebedev Physical Institute, Russian Academy of Science (LPI RAS), Moscow, Russia.